

Article

Increasing the quality factor (Q) of 1D photonic crystal cavity with an end loop-mirror

Mohamad Hazwan Haron ¹, Burhanuddin Yeop Majlis ¹ and Ahmad Rifqi Md Zain ^{1,*}

¹ Institute of Microengineering and Nanoelectronics (IMEN), Universiti Kebangsaan Malaysia; Bangi, 43600, Selangor, Malaysia; rifqi@ukm.edu.my

Abstract: Increasing the quality factor (Q) of an optical resonator device has been a research focus to be utilized in various applications. Higher Q-factor means light is confined in a longer time which will produce a shaper peak and higher transmission. In this paper, we introduce a novel technique to increase further the Q-factor of a one-dimensional photonic crystal (1D PhC) cavity device by using an end loop-mirror (ELM). The technique utilizes and recycles the light transmission from the conventional 1D PhC cavity design. The design has been proved to work by using the 2.5D FDTD simulation with Lumerical FDTD and MODE softwares. By using the ELM technique, the Q- factor of a 1D PhC design has been shown to have increased up to 79.53 % from the initial Q value without the ELM. This novel design technique can be combined with any high Q-factor and very high Q-factor designs to increase more the Q-factor value of a photonic crystal cavity devices or any other suitable optical resonator devices. The experimental result shows that the device is measurable by adding a Y-branch component to the one-port structure and able to get the high-Q result.

Keywords: Photonic crystal cavity; High Q-factor; loss reduction, SOI

1. Introduction

On-chip integrated optical devices have been the research focus solutions for applications such as optical communications, computing system [1], and lab-on-chip bio-sensing [2]. Silicon platform offers a wide range of device and components solutions for integrated designs with silicon-on-insulator (SOI) as the main material. The researches focusing on silicon platform is called silicon photonics. Among the basic passive devices used in PIC design are photonic waveguide (photonic wire) [3], 90° bent waveguide [4], directional coupler [5], Y-branch [6], Mach-Zehnder interferometer (MZI) [7,8], ring resonator [9] and Bragg grating [10,11].

For precise signaling and detection, the important design requirement for the on-chip optical devices is to have a high quality-factor (Q-factor) output. Optical resonator devices such as ring resonator, Bragg grating and photonic crystal are the example of high Q-factor optical devices. High Q-factor devices can be useful for optical biosensing applications which may require a very precise measurement down to a single molecule [12]. This work focuses on one-dimensional photonic crystal (1D PhC) cavity design.

The usual challenges in 1D PhC device researches is to minimize the light losses and utilize the light energy effectively. The usual causes of light losses in photonic crystal devices are from the light scattering at the holes [13,14] and sidewall roughness [15-17]. Sidewall roughness also introduces reflections along the waveguide and phase perturbations [18]. It has been shown that using a wider waveguide at 2 μm can reduce the loss to 0.27 dB/cm [19], however this would introduce a multi-modes condition inside the waveguide. To maintain a single mode condition in the waveguide, 500 nm wide waveguide can be used [20].

The next challenge is to increase the Q-factor. Previous high Q-factor 1D PhC designs used techniques like tapered holes which reduces the modal mismatch effect [21]

and suspended 1D PhC which increases the light confinement due to higher refractive index (RI) contra [22]. However, the weakness of previous 1D PhC designs is the wasted reflected light at the holes which divide the light in two separate directions.

So, if the wasted reflected light can be recycled, making all light reflections at both directions routed to a single direction, the Q-factor and the transmission may be increased. This paper uses this concept to create a novel technique to increase further the Q-factor of a 1D PhC device by utilizing an end loop-mirror (ELM) to harvest the light reflections from one side of the 1D-PhC, and direct it back to the resonance region at the cavity until all light from the harvested side goes back to the incoming light which will result in a higher Q-factor and sharper peak can be obtained.

Although this technique requires the light to be received in the same side as the incoming light source and possess a challenge in the real application design, previous device such as the Michelson interferometer [23] and Micro-ring based laser [24] have shown that it was possible to use the ELM. This suggest that the ELM can also be used to increase the Q-factor of a 1D PhC cavity device.

A custom end loop-mirror design has been used. The design consideration of the loop mirror is to minimize the loss of the light which propagates around the loop, giving even more transmission of light from the loop back to the 1D PhC. Mathematically, it increases the light confinement time inside the cavity and because the Q-factor formula is proportional to the light confinement time, the Q-factor will increase.

The design will be simulated by using Lumerical FDTD and MODE software, and then fabricated by using an electron beam lithography (EBL) based processes. The material of the waveguide will be SOI with 220 nm thickness and 500 nm width. 220 nm is a standard foundry thickness and widely used but does not mean an optimum thickness for all applications [20]. The simulation results showed that the design technique can increase the Q-factor of all selected 1D PhC designs which utilized uniform holes' radius. The experimental result shows that the fabricated one-port device can be measured by adding a Y-branch to the input port and able to get a high-Q transmission. This suggests that this novel design technique can be used to increase other high Q-factor and very high Q-factors PhC designs.

2. 1D PhC modeling and Q-factor simulations

The conventional 1D PhC structure and its geometrical parameters which can be controlled are shown in figure 1. This conventional 1D PhC design uses uniform holes' radius. The usual geometrical parameters which can be controlled on 1D PhC design are the lattice constant (a), cavity length (c), hole radius (r), the number of holes (N), and the width of the waveguide (W).

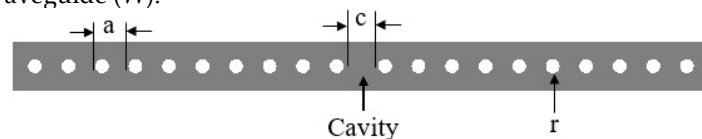


Figure 1. This is a figure. Schemes follow the same formatting.

To find several Q-factor results from the geometrical design changes, the simulation will use 2D FDTD solver with effective index method [25,26], or also known as 2.5D FDTD. This simulation method is faster compared to 3D FDTD simulation which is more useful for final design calculation for device fabrication. It is also more accurate than 2D FDTD which does not calculate the effective index of the material in 2D condition. To calculate the effective index value of the waveguide's parameters used, the Eigenmode solver inside Lumerical MODE software will be used. The waveguide design used is 500 nm wide and 220 nm thick. The simulated effective index (n_{eff}) of the waveguide design from the Eigenmode solver in Lumerical MODE is 2.4445 for fundamental TE. This n_{eff} value will be used in the 2D FDTD solver in Lumerical FDTD software.

The illustration of the simulation setup for the 1D PhC is shown in figure 2. A broadband mode source which has a range from 1.4 to 1.7 μm is used. The design variations will target the wavelength operation at around 1.55 μm . For ideal condition calculation, the light source is put inside the waveguide. The transmission monitor is put after the 1D PhC structure. The Q-factor monitor which will calculate the Q-factor value is put inside the cavity where the resonance is the strongest and will be used for the Q-factor comparison later. The simulations use uniform hole radius of 70 nm.

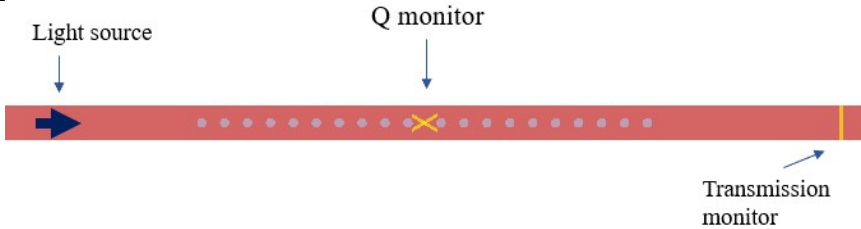


Figure 2. the simulation setup of the 1D PhC.

Several 1D PhC cavity designs are made to calculate and compare their Q-factor values. These designs are simulated with the 2.5D FDTD method. The design details are shown in table 1. Two variations of hole radius were used which were 70 and 50 nm. The waveguide width (W) is 0.5 μm for all designs. The cavity length (c) to get the peak at the middle of the bandgap is around 386 nm. The results that are observed will be the peak wavelength, Q-factor and the transmission (T).

The results of the 2.5D FDTD simulations of the 1D PhC designs and their Q-factor are shown in table 1. The analysis of table 1 will focus the effect of the design variations to the calculate Q-factor. First, increasing the number of holes from 20 to 22 for 70 nm holes increases the Q-factor from 2409 to 4324. This is the same for 50 nm holes, increasing the N from 40 to 46 increases the Q-factor from 8332 to 23881. The W and peak’s wavelength’s effects to the Q-factors are ignored. Comparing the T and Q for each design, it shows that the higher Q comes from the lower T . The conclusion here is the Q-factor can be increased by increasing the N , but will result in lower T . So, there is a trade-off between the Q-factor and the transmission.

Table 1. The simulation results of the 1D PhC and the corresponding Q-factor value.

Design	Radius (nm)	N	a (nm)	Peak Wavelength (nm)	T	Q-factor
A	70	20	367	1550	0.77	2409
B	70	22	367	1550	0.64	4324
C	50	40	358	1550	0.767	8332
E	50	46	358	1550	0.336	23881

The next section will test the insertion of the ELM to increase the Q-factor of each design in table 1.

3. Inserting the end loop-mirror (ELM) and the effect to Q

In this section, a novel technique by using the ELM to increase the Q-factor for each design in table 1 will be tested with the same 2.5D FDTD method shown earlier. The ELM structure used has a radius of 5 μm . The insertion of the ELM’s effect will be observed to the calculated Q-factor and compared with the Q-factor of the 1D-PhC without the ELM.

This observation will determine whether the ELM will be able to increase the Q-factor by increasing the light confinement time inside the cavity. The illustration of the simulation layout of the 1D-PhC with the inserted ELM is shown in figure 3.

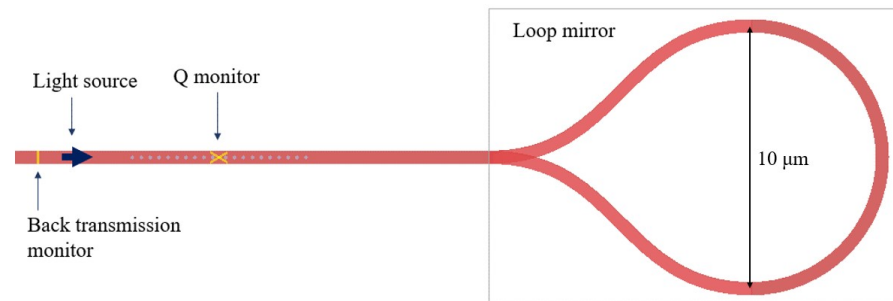


Figure 3. 1D PhC with inserted end loop-mirror structure at one end to increase its Q value and its simulation setup.

The comparison of the 1D PhC structure and the same 1D PhC structure with the ELM structure's transmission spectral are shown in figure 4. The single 1D PhC transmission as shown in figure 4(a) has a peak transmission of 0.636 and Q-factor of 4383, which was calculated by using the Lumerical's Q-factor monitor from the library. The peak transmission for the 1D PhC with the ELM as shown in figure 4(b) has a negative value transmission because the transmission monitor considers the direction of the light propagation, which was taken positive for the direction of the light source propagation. It can be seen the transmission for the 1D PhC with the ELM is higher, and the calculated Q-factor has been increased to 7525. These simulation results are obvious proof that the integration of the ELM can increase the Q-factor of the 1D PhC structure.

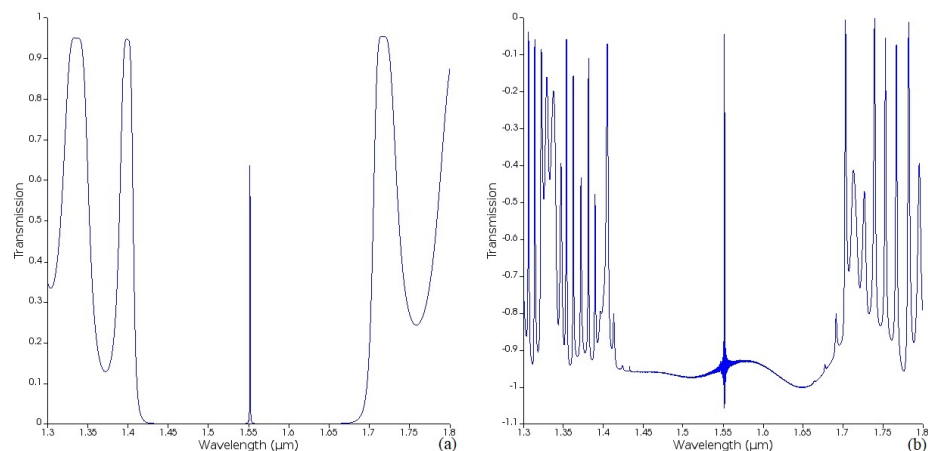


Figure 4. The simulated transmission result of (a) A single 1D PhC and (b) The same 1D PhC with the insertion of the ELM

More simulation results of the new design technique and the resulting Q-factor for design A to D from table 1 are shown in table 2. Analysis of the results in table 2 will focus on the increment of Q-factor after the insertion of the ELM from the initial Q factor without the ELM.

The highest increment of Q-factor in term of percentage is from design A which is by 79.53 %. This is because design A initially has the highest T, which was 0.77, which means more light can be recycled. The Q-factor was increased from 2409 to 4325. The lowest increment is from design D which is by 41.52 %. The reason that design D has 41.52 % improvement, which is the lowest compared to other designs is because it initially has a very low transmission compared to others, which was 0.336. This means that the light amount for reuse from the reflection of the ELM is already low. However, in term of the

value of the Q-factor increment, design D has the highest value which is by 9917. The Q-factor was increased from 23881 to 33808.

Table 2. Improvement of the Q value with the insertion on end loop mirror.

Design	Q without ELM	Q with ELM	Q increment	Improvement percentage (%)
A	2409	4325	1916	79.53
B	4324	7542	3218	74.42
C	8332	14367	6035	72.43
D	23881	33808	9917	41.56

Figure 5 shows the simulation of the electric field (E-field) profile of the 1D PhC with the ELM at the resonance wavelength (1.552 μm). The E-field profile shows that the light has travelled around the ELM and will go back across the 1D PhC structure in backward direction.

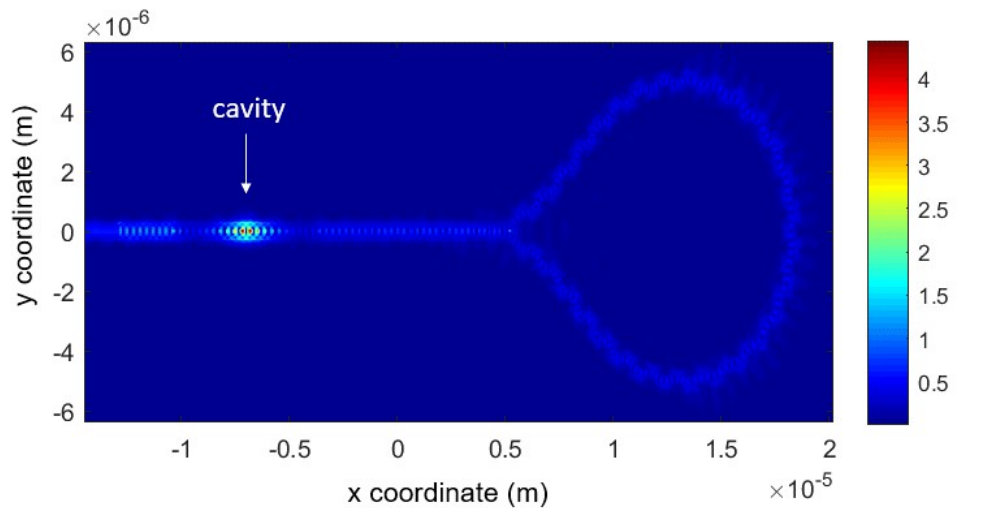


Figure 5. The electric field profile of a 1D PhC cavity structure with an end loop-mirror at resonance frequency.

The simulation results of the Q-factor improvement and the E-field profile have shown that the design concept has worked and should work experimentally. However, because it is a one port device, a correct method must be used to make it measurable. In the experimental part, we show that can be measured by adding a Y-branch to the device.

4. Fabrication and measurement

Because this technique results in one-port structure, it must be shown that it can be measured in the real world by experimentation. Here, we show that this structure is measurable which will make it practical to be used. The fabrication of the device was done by Applied Nanotools Inc. The photonic devices were patterned using a Raith EBPG 5000+ electron beam instrument using a raster step size of 5 nm. The exposure dosage of the design was corrected for proximity effects that result from the backscatter of electrons from exposure of nearby features. Shape writing order was optimized for efficient patterning and minimal beam drift. An anisotropic ICP-RIE etch process was used for the etching. The layout schematic of the device used for measurement is shown in figure 6. It includes the grating couplers to couple light at input and output. A Y-branch

using a SiEPIC PDK component was used to route the light into and out of the 1D PhC with the ELM. The Y-branch is one of the choices to utilize this structure. Other possible components to change the Y-branch is by using the directional coupler or MMI coupler.

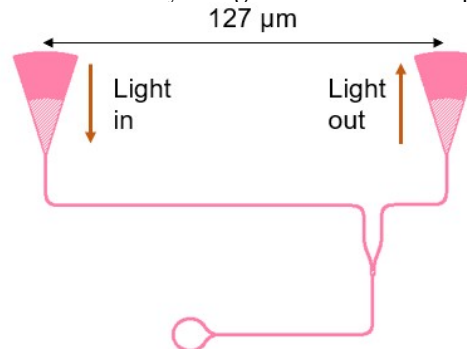


Figure 6. The full layout schematic of the device layout with the input/output component.

The SEM image of one of the fabricated devices is shown in figure 7. The magnification of the SEM image is 2070 times. The focused image shows the 1D PhC structure which is not visible from the larger scale. The holes' size used for the PhC in this image is 70 nm radius which can be done with the EBL process.

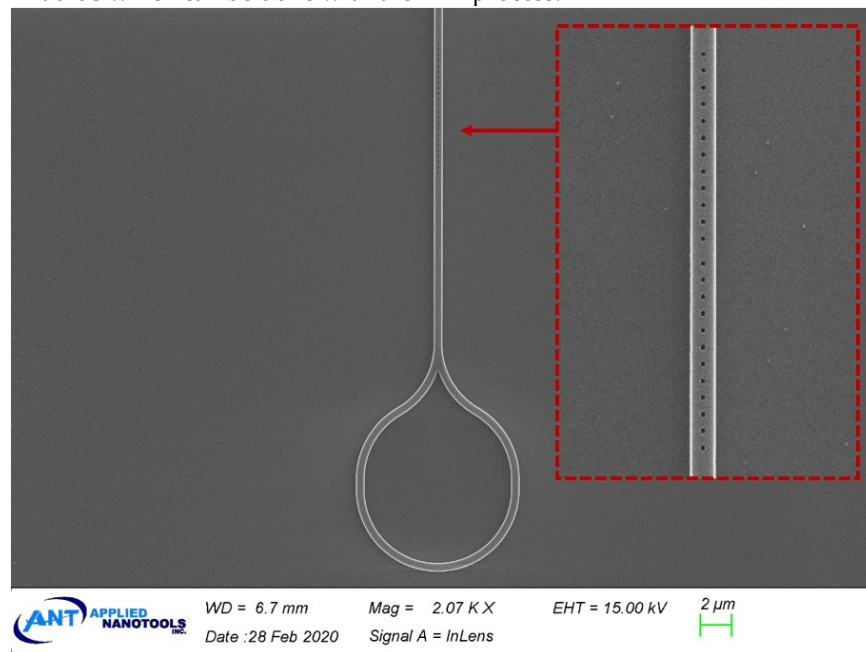


Figure 7. SEM image of the fabricated device.

For the measurement, an Agilent 81600B tunable laser source (TLS) was used as the light source and Agilent 81635A optical power sensors was used as the output sensor. The transmission results are shown in figure 8. The peak is at -37 dB. Note that this transmission includes the insertion loss of a grating coupler times 2, and the 50 % light separation from the Y-branch which results in about 3 dB drop. The transmission includes the grating coupler insertion loss. There is a bit of shift at the peak wavelength from the simulation because of the usage of the 2.5D FDTD method.

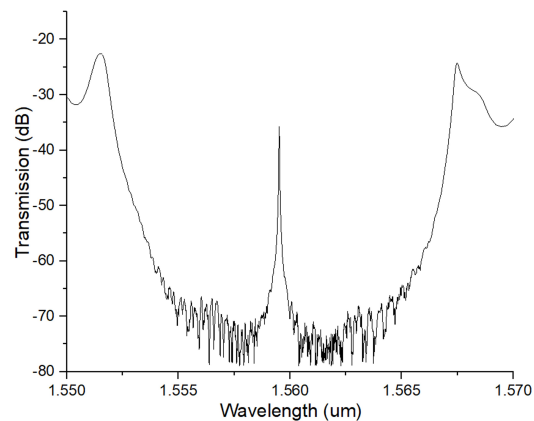


Figure 8. The transmission result from the measurement of the 1D PhC with the end loop mirror.

The experimental result shows that the one-port device can be measured, and the high-Q transmission obtained is as expected. This structure should be more beneficial if there is an array of 1D PhCs used because each array will result in some light wasted which goes into the opposite direction from the transmitted light. Further analysis of this structure could be shown in the future works.

5. Conclusions

The design variations of 1D PhC gave different Q-factor values with the trade-off between the Q-factor and the transmission. A novel design technique has been applied by inserting an end loop-mirror to recycle the light transmission back into the 1D PhC and increases its Q-factor. The light confinement inside the one dimensional photonic crystal cavity devices in term of the Q-factor has been increased by inserting the loop mirror to one end of the device, making the reuse of light transmission from the conventional PhC devices design. This novel technique has been proved theoretically by using FDTD simulation in Lumerical FDTD software. The improvement of the Q-factor from the addition of the end loop-mirror is as high as 79.53 % as shown from the simulation. The experimental result shows that the device is measurable by adding a Y-branch component to the one-port structure and able to get the desired high-Q result.

Author Contributions: Conceptualization, MHH. and ARMZ; methodology, MHH.; software, ARMZ; formal analysis, MHH.; investigation, MHH and ARMZ.; resources, ARMZ.; writing—original draft preparation, MHH.; writing—review and editing, MHH and ARMZ.; supervision, ARMZ; project administration, BYM.; funding acquisition, BYM. All authors have read and agreed to the published version of the manuscript.

Funding: This research was funded by Malaysia Ministry of Higher Education (MOHE) for the support of this work under the FRGS/1/2020/STG02/UKM/02/2.

Data Availability Statement: Data sharing not applicable.

Acknowledgments: We acknowledge Applied Nanotools Inc. for the fabricated device. We also would like to thank Professor Lukas Chrostowski and his team for the development of the SiEPIC PDK.

Conflicts of Interest: The authors declare no conflict of interest.

References

- [1] P. P. Absil, P. Verheyen, P. De Heyn, M. Pantouvaki, and G. Lepage, "Silicon photonics integrated circuits : a manufacturing platform for high density , low power optical I / O ' s," *Opt. Express*, vol. 23, no. 7, pp.

- 9369–9378, 2015.
- [2] J. Song *et al.*, “Silicon-based optoelectronic integrated circuit for label-free bio / chemical sensor,” vol. 21, no. 15, pp. 2528–2533, 2013.
 - [3] E. Dulkeith, F. Xia, L. Schares, W. M. J. Green, and Y. A. Vlasov, “Group index and group velocity dispersion in silicon-on-insulator photonic wires,” *Opt. Express*, vol. 14, no. 9, pp. 1249–1251, 2006.
 - [4] M. Cherchi, S. Ylinen, M. Harjanne, M. Kapulainen, and T. Aalto, “Dramatic size reduction of waveguide bends on a micron-scale silicon photonic platform,” *Opt. Express*, vol. 21, no. 15, pp. 819–821, 2013.
 - [5] A. Prinzen, M. Waldow, and H. Kurz, “Fabrication tolerances of SOI based directional couplers and ring resonators,” *Opt. Express*, vol. 21, no. 14, pp. 21–26, 2013.
 - [6] Y. Zhang *et al.*, “A compact and low loss Y-junction for submicron silicon waveguide,” *Opt. Express*, vol. 21, no. 1, pp. 1310–1316, 2013.
 - [7] T. Mizuno, H. Takahashi, T. Kitoh, M. Oguma, T. Kominato, and T. Shibata, “Mach – Zehnder interferometer switch with a high extinction ratio over a wide wavelength range,” *Opt. Lett.*, vol. 30, no. 3, pp. 251–253, 2005.
 - [8] X. Jiang *et al.*, “Wavelength and bandwidth-tunable silicon comb filter based on Sagnac loop mirrors with Mach- Zehnder interferometer couplers,” *Opt. Express*, vol. 24, no. 3, pp. 555–559, 2016.
 - [9] V. Donzella, A. Sherwali, J. Flueckiger, S. M. Grist, S. T. Fard, and L. Chrostowski, “Design and fabrication of SOI micro-ring resonators based on sub-wavelength grating waveguides,” *Opt. Express*, vol. 23, no. 4, pp. 9103–9112, 2015.
 - [10] P. Prabathan, V. M. Murukeshan, Z. Jing, and P. V. Ramana, “Compact SOI nanowire refractive index sensor using phase shifted Bragg grating,” *Opt. Express*, vol. 17, no. 17, p. 15330, 2009.
 - [11] V. Donzella, A. Sherwali, J. Flueckiger, S. T. Fard, S. M. Grist, and L. Chrostowski, “Sub-wavelength grating components for integrated optics applications on SOI chips,” *Opt. Express*, vol. 22, no. 17, pp. 21037–21050, 2014.
 - [12] F. Vollmer, L. Yang, and S. Fainman, “Label-free detection with high-Q microcavities: A review of biosensing mechanisms for integrated devices,” *Nanophotonics*, vol. 1, no. 3–4, pp. 267–291, 2012.
 - [13] P. Velha *et al.*, “Ultra-high-reflectivity photonic-bandgap mirrors in a ridge SOI waveguide,” *New J. Phys.*, vol. 8, 2006.
 - [14] P. C. Waveguides, A. Ebnali-heidari, C. Prokop, M. Ebnali-heidari, and C. Karnutsch, “A Proposal for Loss Engineering in Slow-Light,” *J. Light. Technol.*, vol. 33, no. 9, pp. 1905–1912, 2015.
 - [15] T. Street, “A theoretical analysis of scattering loss from planar optical waveguides,” *Opt. Quantum Electron.*, vol. 26, pp. 977–986, 1994.
 - [16] I. Waveguides *et al.*, “Radiation Modes and Roughness Loss in High Index-Contrast Waveguides,” *IEEE J. Sel. Top. Quantum Electron.*, vol. 12, no. 6, pp. 1306–1321, 2006.
 - [17] K. P. Yap *et al.*, “SOI Waveguide Fabrication Process Development Using Star Coupler Scattering Loss Measurements,” in *Proceedings of SPIE - The International Society for Optical Engineering*, 2008, vol. 6800, pp. 1–12.
 - [18] A. D. Simard, N. Ayotte, Y. Painchaud, and S. Larochelle, “Impact of Sidewall Roughness on Integrated Bragg Gratings,” vol. 29, no. 24, pp. 3693–3704, 2011.
 - [19] P. Dong *et al.*, “Low loss shallow-ridge silicon waveguides,” *Opt. Express*, vol. 18, no. 14, pp. 4752–4757, 2010.
 - [20] D. Xu *et al.*, “Silicon Photonic Integration Platform — Have We Found the Sweet Spot?,” *IEEE J. Sel. Top. Quantum Electron.*, vol. 20, no. 4, 2014.
 - [21] A. R. Md Zain, M. Gnan, H. M. H. Chong, M. Sorel, and R. M. De La Rue, “Tapered photonic crystal

-
- microcavities embedded in photonic wire waveguides with large resonance quality-factor and high transmission," *IEEE Photonics Technol. Lett.*, vol. 20, no. 1, pp. 6–8, 2008.
- [22] H. Q. Photonic *et al.*, "High Quality-Factor 1-D-Suspended Photonic Crystal/Photonic Wire Silicon Waveguide Micro-Cavities," *IEEE Photonics Technol. Lett.*, vol. 21, no. 24, pp. 1789–1791, 2009.
- [23] J. Song *et al.*, "Fast and low power Michelson interferometer thermo-optical switch on SOI Abstract :," *Opt. Express*, vol. 16, no. 20, pp. 15304–15311, 2008.
- [24] Y. Zhang *et al.*, "Sagnac loop mirror and micro-ring based laser cavity for silicon-on-insulator," *Opt. Express*, vol. 22, no. 15, pp. 1096–1101, 2014.
- [25] M. Hammer and O. V Ivanova, "Effective index approximations of photonic crystal slabs : a 2-to-1-D assessment," *Opt. Quantum Electron.*, vol. 41, pp. 267–283, 2009.
- [26] H. G. Danielmeyer, W. Streifer, D. R. Scifres, G. Fonstad, and T. Oaks, "The Effective Index Method and Its Application to Semiconductor Lasers," *IEEE J. Quantum Electron.*, no. 7, pp. 1083–1089, 1982.